Macromolecules

pubs.acs.org/Macromolecules Article

Synthesis of Degradable Homopolymer, Gradient and Block Copolymers, and Self-Assembly via RAFT Polymerization of 4,4-Dimethyl-2-methylene-1,3-dioxolan-5-one

Tze Kwang Gerald Er, Xuan Yong Haydon Lim, Xin Yi Oh, and Atsushi Goto*

Cite This: *Macromolecules* 2024, 57, 8983–8997 Read Online

ACCESS | Metrics & More | Article Recommendations | Supporting Information

ABSTRACT: Reversible addition−fragmentation chain transfer polymerizations of 4,4-dimethyl-2-methylene-1,3-dioxolan-5-one (DMDL) were conducted to yield degradable polymers with low dispersities. As well as homopolymers, random copolymers and block copolymers were synthesized by combining DMDL with various hydrophobic and hydrophilic monomers such as (functional) methacrylates, acrylates, and acrylamides, which are the so-called "more activated" monomers, and vinyl acetate and vinylpyrrolidone, which are the so-called "less activated" monomers. The obtained polymers were demonstrated to degrade under basic conditions. In the studied systems, random polymerization tended to yield gradient copolymers shifting from comonomer-rich segments to DMDL-rich segments, owing to the largely different reactivities of DMDL and comonomers. Such gradient copolymers may exhibit properties similar to those of block copolymers. Gradient copolymers with hydrophilic vinylpyrrolidone segments and hydrophobic DMDL-rich segments were synthesized and used to generate self-assemblies, i.e., micelles and vesicles, in water. The generated self-assemblies were demonstrated to degrade under basic conditions.

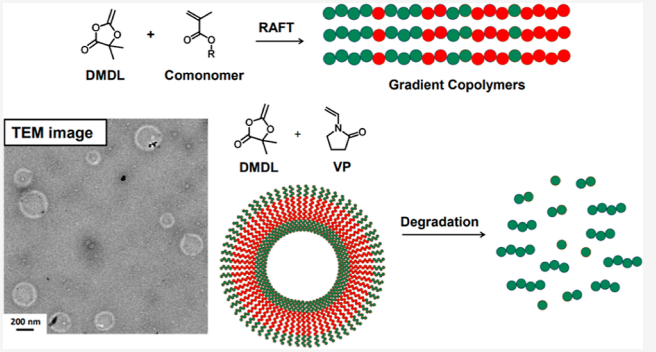

INTRODUCTION

Degradable polymers have attracted growing attention due to the growing use of plastics.[1−3] Synthetic polymers are usually difficult to degrade, leading to research for more sustainable polymers that can degrade upon stimuli. Besides sustainability aspects, degradable polymers are used for stimuli-responsive degradable materials in, e.g., delivery systems. Various degradable polymer particles and capsules have been developed,[4,5] where degradation of the polymer was used for the release mechanism.

Polyesters and polycarbonates are widely used as degradable synthetic polymers, as they have hydrolyzable backbones for degradation.[6−10] Polymers synthesized via radical polymerization are usually difficult to degrade because their backbones consist of aliphatic carbon−carbon bonds. In order to provide hydrolyzable bonds in backbones, cyclic ketene acetals (CKAs) have been used as monomers in radical polymerization.[11−19] The ring opening of CKAs during the polymerization generates hydrolyzable ester linkages in backbones. Random copolymerizations of CKAs with various vinyl monomers have been widely studied, providing a range of degradable copolymers. Living radical polymerization, also termed reversible deactivation radical polymerization, has also been used for CKAs, generating various random and block copolymers with low dispersities.[13,14,17−19] The obtained random and block copolymers were used for, e.g., degradable coatings,[20] photolithographic films,[21,22] and biomedical materials.[23,24]

Our research group recently used 4,4-dimethyl-2-methylene-1,3-dioxolan-5-one (DMDL) (Scheme 1a) as a monomer to generate degradable polymers via conventional radical polymerization.[25] DMDL is a 5-membered cyclic monomer and can generate its homopolymer and random copolymers with a range of vinyl monomers.[25] Unlike CKAs, the ring of DMDL is not opened but retained in the polymerization (Scheme 1a), yielding ring-retained polymers. The obtained polymers can degrade under basic conditions. Scheme 1b shows a possible degradation mechanism. The backbone scission can occur at a point at which two DMDL units are successively sequenced. First, a hydroxide (OH^-) ion attacks the carbonyl group (C═O) at the hemiacetal ester (compound **1** in Scheme 1b), generating an alkoxide anion (compound **2**). The subsequent elimination can lead to backbone scission to generate two polymer chains bearing a

Received: July 16, 2024
Revised: September 13, 2024
Accepted: September 18, 2024
Published: September 27, 2024

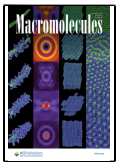

https://doi.org/10.1021/acs.macromol.4c01638
Macromolecules 2024, 57, 8983−8997

Scheme 1. (a) Polymerization of DMDL and (b) Possible Degradation Mechanism of DMDL-Containing Polymer

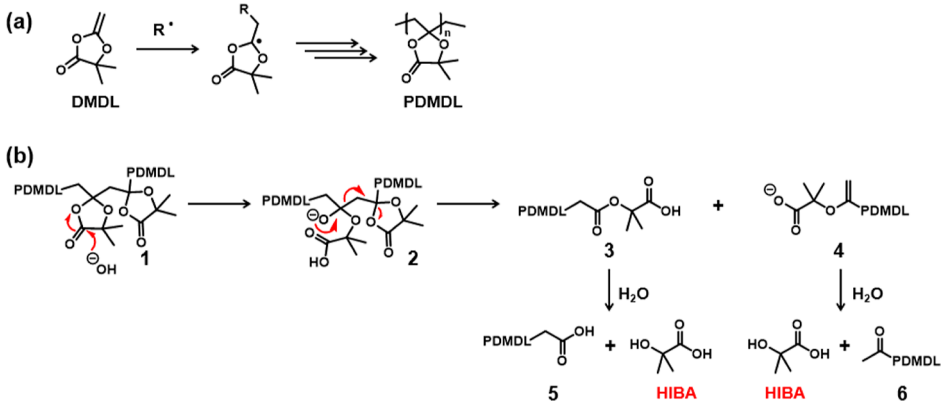

Scheme 2. RAFT Process

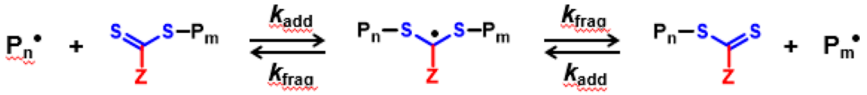

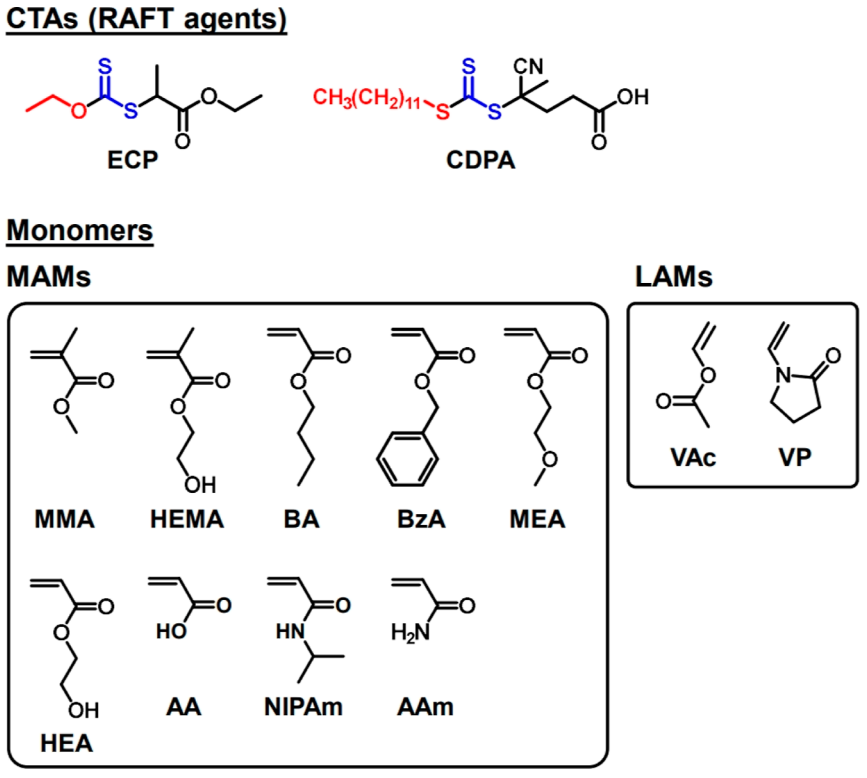

Figure 1. CTAs (RAFT agents) and monomers (besides DMDL (Scheme 1)) used in this work. MAMs and LAMs refer to more active monomers and less active monomers, respectively.

carboxylic acid (compound **3**) and a carboxylate (compound **4**), which can further degrade into polymer chains bearing a carboxylic acid (compound **5**) and a ketone (compound **6**) and 2-hydroxyisobutyric acid (HIBA). As a useful aspect, HIBA is an ingredient of DMDL (monomer). HIBA can be collected and reused to synthesize DMDL, whereby four of the six carbons of DMDL are recyclable.

In the present work, instead of conventional radical polymerization,[25] we used reversible addition−fragmentation chain transfer (RAFT) polymerization to synthesize homopolymers and copolymers of DMDL with well-defined structures. Scheme 2 shows the RAFT process,[26−36] where P_m−SCSZ is a polymer dormant species. The propagating radical ($P_n^•$) undergoes the addition to P_m−SCSZ, generating an intermediate radical (P_n-SC·ZS−P_m). The intermediate radical subsequently undergoes fragmentation, forming a polymer dormant species (P_n−SCSZ) and a propagating radical ($P_m^•$). Through addition and fragmentation processes, chain transfer between the propagating radical ($P_n^•$) and the dormant species (P_m−SCSZ) completes. To ensure frequent chain transfer, the C═S bond of the dormant species must be sufficiently reactive for the addition of the propagating radical. Also, the

https://doi.org/10.1021/acs.macromol.4c01638
Macromolecules 2024, 57, 8983−8997

Table 1. Homopolymerizations of DMDL

entry	CTA	$[DMDL]_0/[CTA]_0/[AIBN]_0$ (equiv)[a]	T (°C)	t (h)	conv. (%)[b]	M_n[c] ($M_{n,theo}$[d])	$Đ$[c]
1	ECP	100/1/0.2	70	24	61	4900 (8000)	1.18
2	ECP	200/1/0.2	70	24	70	8300 (18,000)	1.28
3	CDPA	100/1/0.2	70	24	57	5600 (7700)	1.24
C1	None	200/0/0.2	70	24	77	9200	1.53

[a]Solution polymerization in DMF (70 wt %) with 30 wt % of DMDL. [b]Monomer conversions determined with ^{1}H NMR. [c]PMMA-calibrated GPC values (THF eluent). [d]Theoretical M_n calculated according to ($[DMDL]_0/[CTA]_0$) × (monomer conversion) × (molecular weight of DMDL) + (molecular weight of CTA).

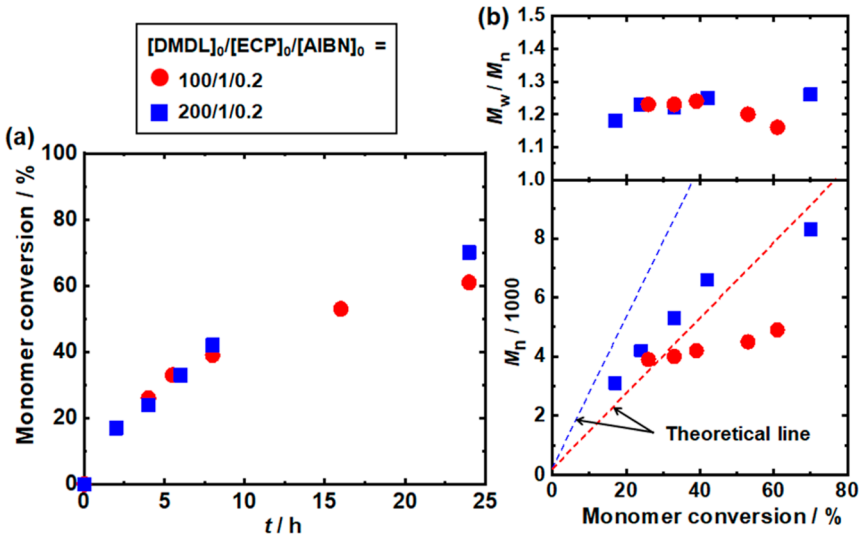

Figure 2. Plots of (a) monomer conversion vs. polymerization time (t) and (b) M_n and M_w/M_n vs monomer conversion for the DMDL/ECP/AIBN system (70 °C); $[DMDL]_0/[ECP]_0/[AIBN]_0$ = 100/1/0.2 (equiv) (Table 1, entry 1) and 200/1/0.2 (equiv) (Table 1, entry 2). The symbols are indicated in the figure.

intermediate radical must undergo fragmentation sufficiently rapidly. Otherwise, the intermediate radical accumulates, and termination between the intermediate radical and propagating radical and termination between the two intermediate radicals can be significant, causing a retardation in the polymerization rate and a significant generation of dead polymer chains.[37,38]

Figure 1 shows the chain transfer agents (CTAs) (RAFT agents) and monomers studied in the present work. We synthesized homopolymers, gradient copolymers, and block copolymers via RAFT polymerization, the latter two of which are not accessible via conventional radical polymerization. Gradient copolymers are obtainable via living radical random copolymerizations when one monomer is more reactive than the other monomer[39−41] because a history of the monomer consumption of the two monomers is recorded on each polymer chain; namely, the more reactive monomer will tend to be added in the early polymer sequence, and the less reactive monomer will tend to be added later, forming a gradient copolymer. Vinyl monomers are classified into "more activated" monomers (MAMs) and "less activated" monomers (LAMs) based on the stability of the generated propagating radical. MAMs generally bear conjugated substituents on the polymerizable vinyl group and generate stabilized propagating radicals, while LAMs generally do not bear conjugated substituents and generate less stabilized propagating radicals. DMDL bears no conjugated substituents but two non-conjugated (ether) substituents and is considered as a LAM. We carried out RAFT random copolymerizations of DMDL (LAM) with several MAMs and LAMs as comonomers and studied composition gradients in those LAM-MAM and LAM−LAM random copolymerizations. We studied the base-assisted degradation of the obtained gradient copolymers. As an application, we formed self-assemblies of degradable gradient copolymers. We synthesized amphiphilic gradient copolymers with hydrophobic (DMDL) and hydrophilic segments, used them to form micelles and vesicles, and demonstrated base-assisted degradation of the micelles and vesicles for possible applications as degradable delivery containers.

RESULTS AND DISCUSSION

Homopolymerizations of DMDL. We carried out RAFT homopolymerizations of DMDL using two different CTAs (Figure 1), i.e., ethyl 2-[(ethoxycarbonothioyl)thio]propionate (ECP) (Z = *O*-alkyl) and 4-cyano-4-[[(dodecylthio)-carbonothioyl]thio]pentanoic acid (CDPA) (Z = *S*-alkyl). We heated a mixture of DMDL (100 equiv), ECP (1 equiv), and 2,2′-azoisobutyronitrile (AIBN) (0.2 equiv) as a conventional radical initiator at 70 °C (Table 1, entry 1). The monomer conversion reached 61% (as determined with ^{1}H NMR) for 24 h, yielding a poly(4,4-dimethyl-2-methylene-1,3-dioxolan-5-one) (PDMDL) with M_n = 4900 and $Đ$ (= M_w/M_n) = 1.18, where M_n and M_w are the number- and weight-average molecular weights, respectively, and $Đ$ is dispersity. The M_n and $Đ$ values are not absolute values but PMMA-calibrated gel permeation chromatography (GPC) values, where PMMA is poly(methyl methacrylate). Figure 2 (red circles) shows the polymerization behavior. The monomer conversion increased

https://doi.org/10.1021/acs.macromol.4c01638
Macromolecules 2024, 57, 8983−8997

with an increase in time (Figure 2a (red circles)), and the M_n value increased with an increase in the monomer conversion (Figure 2b (red circles)). The deviation of the M_n value from the theoretical value is ascribed to the PMMA-calibrated GPC values. The $Đ$ value was 1.18−1.24 throughout the polymerization. Thus, relatively low-dispersity PDMDLs were obtained.

Figure 3 shows the ^{1}H NMR spectrum ($CDCl_3$) of the PDMDL obtained at 5.5 h of polymerization (monomer conversion = 33%) and purified by reprecipitation in a hexane/diethyl ether mixture (1/1 (v/v)) (nonsolvent) (M_n = 4500 and $Đ$ = 1.14). The integration ratio of methylene (CH_2) protons (*a*) of PDMDL (and methine (CH) proton (*c*) of ECP) appearing at 2.2−3.2 ppm and methylene (CH_2) protons (*e*) of ECP appearing at 4.1−4.2 ppm suggests the number of DMDL monomer units per ECP to be 34, which is close to the theoretical degree of polymerization of 33 (=$[DMDL]_0/[ECP]_0$ × (monomer conversion)). The result suggests a high initiation efficiency of ECP (approximately 97% (=33/34)) in the homopolymerization of DMDL. The amount of new chains formed from AIBN was relatively minor in this NMR study, as we used 0.2 equiv of AIBN to ECP, approximately 52% of AIBN decomposes at 70 °C for 5.5 h,[42] AIBN generates two radicals, and the initiation efficiency of AIBN is typically 0.5−0.6,[43] which suggests that the amount of new chains formed from AIBN was ca. 0.10−0.12 equiv. (=(0.2 equiv) × (52%) × 2×(0.5−0.6)) to that of the chains formed from ECP. Thus, the fraction of the dead polymer chain would be 9−11% (=0.10/1.10−0.12/1.12).

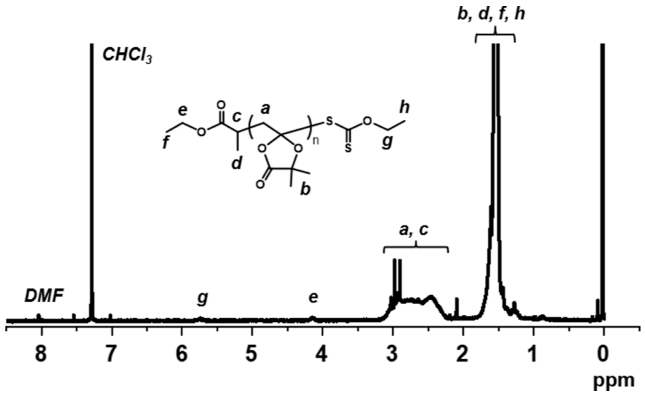

Figure 3. ^{1}H NMR ($CDCl_3$) spectrum of PDMDL synthesized in the DMDL/ECP/AIBN system (Table 1, entry 1) at 5.5 h of polymerization (monomer conversion = 33%) and purified by reprecipitation (M_n = 4500 and $Đ$ = 1.14).

In Figure 2b, we observed a deviation of the M_n value from the theoretical value, which is ascribed to the use of PMMA-calibrated GPC (as mentioned) and also the formation of the new chains from AIBN. New chains were formed, and hence the averaged molecular weight (M_n) value increased relatively slowly with an increase in the monomer conversion. After 8 h, both monomer conversion (Figure 2a) and M_n value (Figure 2b) only slowly increased because 84% of AIBN already decomposes for 8 h.[42]

We increased the $[DMDL]_0/[ECP]_0$ ratio from 100 (Table 1, entry 1 and Figure 2 (red circles)) to 200 (Table 1, entry 2 and Figure 2 (blue squares)) to target higher molecular weight polymers. As expected, the M_n value after 24 h increased from 4900 (at the $[DMDL]_0/[ECP]_0$ ratio = 100) to 8300 with a slightly larger $Đ$ value of 1.28 at the $[DMDL]_0/[ECP]_0$ ratio = 200.

As a comparison experiment, we carried out a conventional radical polymerization of DMDL without using CTA (ECP) (Table 1, entry C1), which generated a polymer with a relatively large $Đ$ value (=1.53) for 24 h. The result shows that the observed relatively low $Đ$ value (Table 1, entry 2) was afforded by the use of CTA (RAFT polymerization).

The use of CDPA as a CTA (Table 1, entry 3 and Figure S1 in Supporting Information) exhibited similar polymerization behavior but resulted in a slightly slower polymerization and a slightly larger $Đ$ value than the use of ECP. The monomer conversion reached 57% for 24 h, yielding a PDMDL with M_n = 5600 and $Đ$ = 1.24 (Table 1, entry 3). The slightly slower polymerization and larger $Đ$ value would be ascribed to the slightly slow initiation from CDPA. The radical generated from CDPA is a highly stabilized tertiary alkyl radical $^{\bullet}C(CH_3)(CN)(COOH)$ with two conjugated groups and would be too stable to add DMDL (monomer) effectively. The radical from CDPA would tend to undergo termination with another radical, resulting in a slower polymerization and broader molecular weight distribution. Another possible minor reason is a possibly slow fragmentation of the intermediate radical and thereby terminations involving the intermediate radical for the combination of CDPA and the LAM monomer (DMDL), as described below. Nevertheless, both ECP and CDPA were efficient for the homopolymerization of DMDL, while ECP was slightly preferred.

Random Copolymerizations of DMDL. We studied random copolymerizations of DMDL and comonomers. The studied comonomers (Figure 1) were methacrylates (methyl methacrylate (MMA) and hydroxyethyl methacrylate (HEMA)), acrylates (butyl acrylate (BA), benzyl acrylate (BzA), methoxyethyl acrylate (MEA), hydroxyethyl acrylate (HEA), and acrylic acid (AA)), and acrylamides (*N*-isopropylacrylamide and acrylamide (AAm)), which are MAMs (conjugated monomers), and vinyl acetate (VAc) and vinylpyrrolidone (VP), which are LAMs (nonconjugated monomers). We heated a mixture of DMDL (50 equiv), comonomer (50 equiv), CTA (1 equiv), and AIBN (0.2 equiv) at 70 °C for 24 h (Table 2). We fixed 24 h for a comparison purpose in different copolymerizations. The half-life of AIBN is approximately 5 h at the studied temperature of 70 °C. After 24 h, a majority (approximately 99.6%)[42] of AIBN would be consumed, and the polymerization would be very slow even if the polymerization continued. The (initial) monomer composition was 50% for DMDL and 50% for the comonomer. For the CTA, we used CDPA for MAMs and ECP for LAMs. The reactivity of the C═S bond in the CTA largely depends on the *Z* group (Scheme 2).[44,45] When the *Z* group stabilizes the intermediate radical better, the addition rate constant (k_{add} (Scheme 2)) increases, resulting in a more frequent chain transfer. The k_{add} value increases in the order of Z = *O*-alkyl (ECP) < *S*-alkyl (CDPA), and hence we used CDPA for MAMs (Table 2, entries 1−9). However, for LAMs, the propagating radical is a "less stable" radical, and hence, the intermediate radical can be more stable than the propagating radical, resulting in an accumulation of the intermediate radical and causing terminations involving the intermediate radical. Thus, a less stabilized *Z* group is required to destabilize the intermediate radical (promote fragmentation), and hence, we used ECP (Z = *O*-alkyl) for LAMs (Table 2, entries 10 and 11).

https://doi.org/10.1021/acs.macromol.4c01638
Macromolecules 2024, 57, 8983−8997

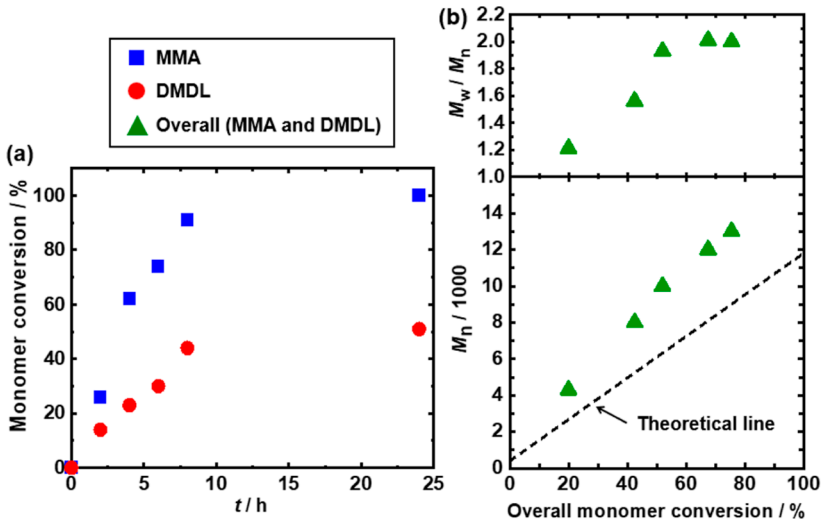

Figure 4. Plots of (a) monomer conversion vs. time (t) and (b) M_n and M_w/M_n vs overall monomer conversion for the MMA/DMDL/CDPA/AIBN system (70 °C) (Table 2, entry 1): $[DMDL]_0/[DMDL]_0/[ECP]_0/[AIBN]_0$ = 50/50/1/0.2 (equiv). The symbols are indicated in the figure. In (b), the overall monomer conversion is (conversion of DMDL) × 0.5 + (conversion of comonomer (MMA)) × 0.5.

Table 2. Random Copolymerizations of DMDL and Comonomer (M)

entry	comonomer (M)	CTA	$[M]_0/[DMDL]_0/[CTA]_0/[AIBN]_0$[a] (equiv)	T (°C)	t (h)	conv.[b] (M/DMDL) (%/%)	overall conv.[c] (%)	M_n[d] ($M_{n,theo}$[e])	$Đ$[d]	F_{DMDL} (%)[f]
1	MMA	CDPA	50/50/1/0.2	70	24	100/52	76	13000 (8700)	2.01	34
2	HEMA	CDPA	50/50/1/0.2	70	24	100/78	89	21000 (12000)	2.01	44
3	BA	CDPA	50/50/1/0.2	70	24	99/78	89	12000 (12000)	1.39	44
4	BzA	CDPA	50/50/1/0.2	70	24	100/76	88	8400 (13000)	1.47	42
5	MEA	CDPA	50/50/1/0.2	70	24	100/73	87	10000 (12000)	1.44	42
6	HEA	CDPA	50/50/1/0.2	70	24	100/99	100	11000 (13000)	1.34	50
7	AA	CDPA	50/50/1/0.2	70	24	0/0	0	NA	NA	NA
8	NIPAm	CDPA	50/50/1/0.2	70	24	100/67	84	14000 (10000)	1.32	40
9	AAm	CDPA	50/50/1/0.2	70	24	NA/NA[g]	NA	NA	NA	NA
10	VAc	ECP	50/50/1/0.2	70	24	100/60	80	5100 (8400)	1.23	38
11	VP	ECP	50/50/1/0.2	70	24	53/30	42	3400 (5100)	1.19	36
12	VAc	CDPA	50/50/1/0.2	70	24	50/40	45	3800 (5100)	1.33	44
13	VP	CDPA	50/50/1/0.2	70	24	24/17	21	<1000[h] (2800)	NA[h]	NA[i]

[a]Solution polymerization in DMF (70 wt %) with 30 wt % of monomers in total. [b]Monomer conversions of comonomer (M) and DMDL determined with ^{1}H NMR. [c]Overall monomer conversion of the two monomers calculated according to (conversion of DMDL) × (initial fraction of DMDL (0.5)) + (conversion of comonomer) × (initial fraction of comonomer (0.5)). [d]PMMA-calibrated GPC values (DMF eluent). [e]Theoretical M_n calculated according to ($[monomers]_0/[CTA]_0$) × (monomer conversion) × (molecular weight of monomer) + (molecular weight of CTA). [f]Fraction of DMDL calculated from the monomer conversions of DMDL and comonomer. [g]Insoluble polymer gel was generated. [h]The molecular weight was too low to accurately determine the M_n and $Đ$ values using GPC. [i]The molecular weight was too low to collect the entire polymer (oligomer).

The random copolymerization with MMA yielded a PMMA-*r*-PDMDL (M_n = 13000, $Đ$ = 2.01, and F_{DMDL} = 34%) for 24 h (Table 2, entry 1), where F_{DMDL} is the fraction of DMDL in the copolymer. The F_{DMDL} value was calculated from the monomer conversions (monomer consumptions) of DMDL and the comonomer (MMA). Figure 4a shows the plots of monomer conversion vs time for DMDL (red circle) and MMA (blue square). The monomer reactivity ratios of DMDL and MMA were previously determined to be r_{MMA} = 4.60 and r_{DMDL} = close to zero (70 °C),[25] which means that MMA is much more reactive than DMDL. Thus, MMA was consumed much faster than DMDL (Figure 4a). Conventional radical polymerization can yield a mixture of MMA-rich polymer chains (that can be generated at an early stage of polymerization) and DMDL-rich polymer chains (that can be generated at a later stage of polymerization). In contrast, as mentioned, in the RAFT polymerization, each polymer chain can contain a MMA-rich sequence (initial segment of the

https://doi.org/10.1021/acs.macromol.4c01638
Macromolecules 2024, 57, 8983−8997

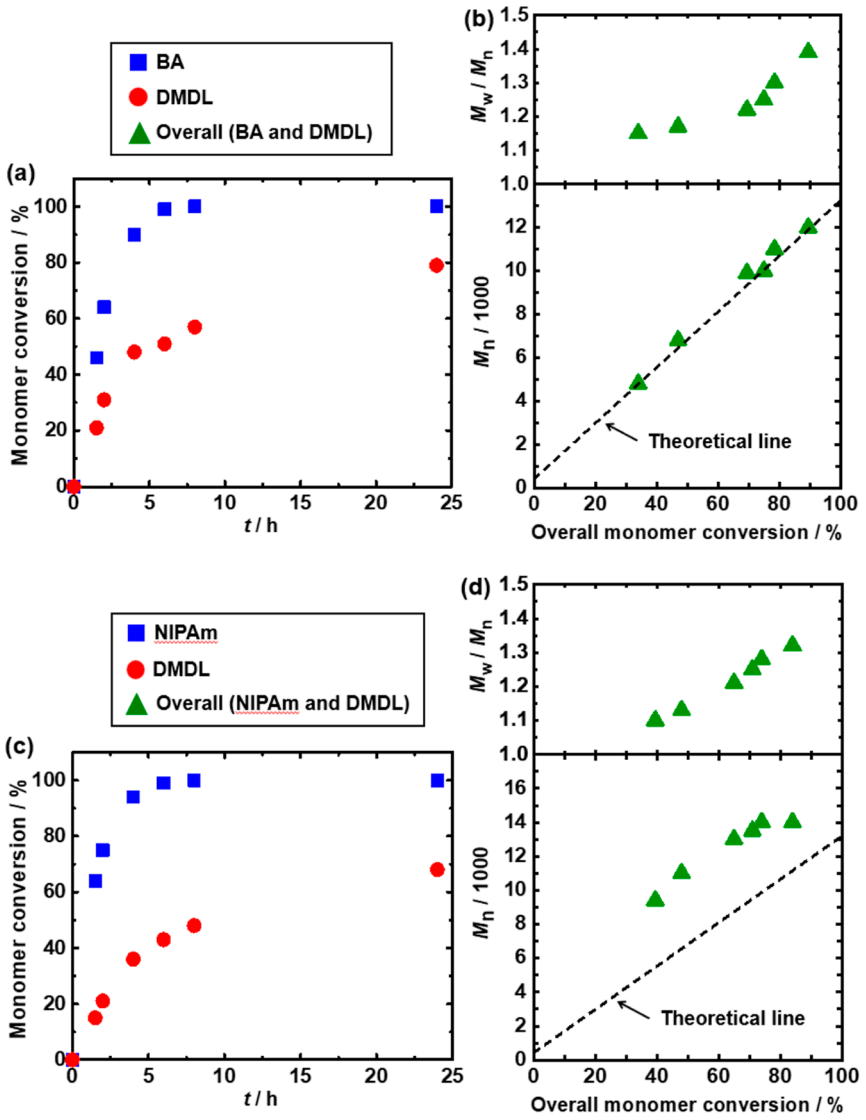

Figure 5. Plots of (a) monomer conversion vs. time (t) and (b) M_n and M_w/M_n vs overall monomer conversion for the BA/DMDL/CDPA/AIBN system (70 °C) (Table 2, entry 3): $[BA]_0/[DMDL]_0/[CDPA]_0/[AIBN]_0$ = 50/50/1/0.2 (equiv). Plots of (c) monomer conversion vs time (t) and (d) M_n and M_w/M_n vs overall monomer conversion for the NIPAm/DMDL/CDPA/AIBN system (70 °C) (Table 2, entry 8): $[NIPAm]_0/[DMDL]_0/[CDPA]_0/[AIBN]_0$ = 50/50/1/0.2 (equiv). The symbols are indicated in the figure. In (b,d), the overall monomer conversion is (conversion of DMDL) × 0.5 + (conversion of comonomer) × 0.5.

chain) and a DMDL-rich sequence (end segment of the chain), forming a gradient copolymer because of the significantly different reactivities of MMA and DMDL. The evolution of the F_{DMDL} value vs the overall monomer conversion is given in Figure S2 in Supporting Information. Figure 4b shows the plots of M_n and $Đ$ vs the overall monomer conversion of MMA and DMDL. The M_n value increased with an increase in the overall monomer conversion. The $Đ$ value was relatively low (~1.5) up to approximately 40% overall monomer conversion and increased to 2.01 at 76% overall monomer conversion (for 24 h). The large $Đ$ value would be ascribed to the actual broad molecular weight distribution and might also be partly ascribed to variation in the monomer composition (different hydrodynamic volumes or swelling) among the generated polymer chains. The copolymerization with HEMA, which is a functional methacrylate with a hydroxyl group, yielded a PHEMA-*r*-PDMDL (M_n = 21000, $Đ$ = 2.01, and F_{DMDL} = 44%) with an 89% overall monomer conversion for 24 h (Table 2, entry 2 and Figure S3 in Supporting Information), where PHEMA is poly(2-hydroxyethyl methacrylate). Thus, we obtained gradient copolymers of DMDL and methacrylates at relatively high overall monomer conversions (76−89%), although the $Đ$ values were relatively large (approximately 2.0). The increase in the $Đ$ value with an increase in the overall monomer conversion would be ascribed to an inefficient exchange (an inefficient RAFT) of DMDL-terminal dormant species with a methacrylate-terminal propagating radical. The dormant state is prolonged for DMDL-terminal dormant species, and hence DMDL-terminal dormant species is gradually accumulated over time (at different chain lengths), which would broaden the molecular weight distribution.

The copolymerization with BA, which is another family of monomers (acrylate), yielded a PBA-*r*-PDMDL (M_n = 12000, $Đ$ = 1.39, and F_{DMDL} = 44%) with an 89% overall monomer conversion (Table 2, entry 3), where PBA is poly(butyl acrylate). Similar to MMA (methacrylate), the comonomer BA was consumed faster than DMDL (Figure 5a). The monomer

https://doi.org/10.1021/acs.macromol.4c01638
Macromolecules 2024, 57, 8983−8997

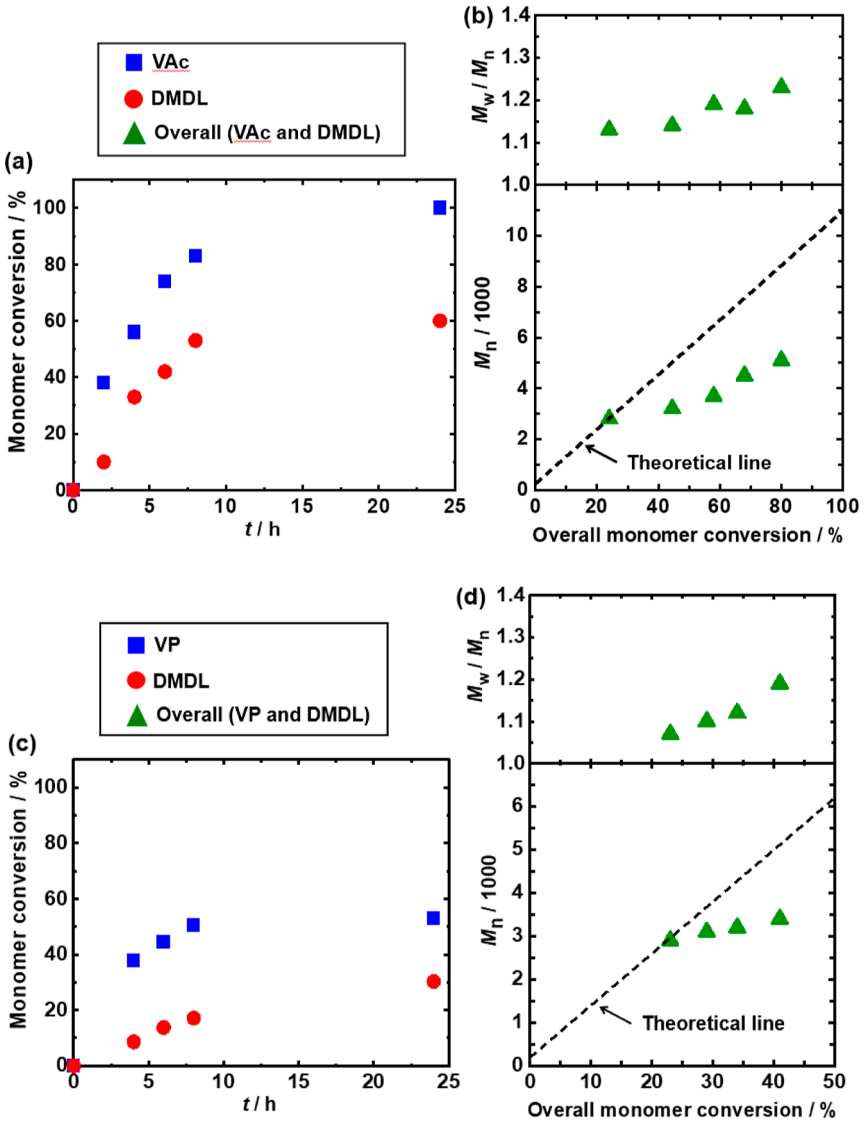

Figure 6. Plots of (a) monomer conversion vs. time (t) and (b) M_n and M_w/M_n vs. overall monomer conversion for the VAc/DMDL/ECP/AIBN system (70 °C) (Table 2, entry 10): $[VAc]_0/[DMDL]_0/[ECP]_0/[AIBN]_0$ = 50/50/1/0.2 (equiv). Plots of (c) monomer conversion vs. time (t) and (d) M_n and M_w/M_n vs overall monomer conversion for the VP/DMDL/ECP/AIBN system (70 °C) (Table 2, entry 11): $[VP]_0/[DMDL]_0/[ECP]_0/[AIBN]_0$ = 50/50/1/0.2 (equiv). The symbols are indicated in the figure. In (b,d), the overall monomer conversion is (conversion of DMDL) × 0.5 + (conversion of comonomer) × 0.5.

reactivity ratios of BA and DMDL are r_{BA} = 0.83 and r_{DMDL} = 0.03, while those of MMA and DMDL are r_{MMA} = 4.60 and r_{DMDL} = close to zero.[25] These values mean that the BA/DMDL system (r_{BA} = 0.83) has a more alternating tendency than the MMA/DMDL system (r_{MMA} = 4.60). Thus, the BA/DMDL system would tend to generate a gradient copolymer but with a more randomly distributed monomer sequence. The M_n value increased with an increase in the overall monomer conversion, and the $Đ$ value was relatively low (1.15−1.39) throughout the polymerization up to an 89% overall monomer conversion (Figure 5b). Copolymerizations with functional acrylates, i.e., BzA with a benzyl group, MEA with a methoxyethyl group, and HEA with a hydroxyl group, also yielded relatively low-dispersity random (gradient) copolymers with M_n = 8400−11000, $Đ$ = 1.34−1.47, and F_{DMDL} = 42−50% with 87−100% overall monomer conversions for 24 h (Table 2, entries 4−6 and Figures S4−S6 in Supporting Information). Similar to the acrylates, the copolymerization with NIPAm, which is another family of MAM, yielded a low-dispersity random (gradient) copolymer with M_n = 14000, $Đ$ = 1.32, and F_{DMDL} = 40% with an 84% overall monomer conversion (Table 2, entry 8, and Figure 5c,d). Thus, we obtained (relatively) low-dispersity copolymers using BA, functional acrylates, and a functional AAm. We also studied nonprotected AA (AA with a carboxylic acid) and AAm (AAm with an amide) (Table 2, entries 7 and 9). For AA, no polymerization occurred. Several unknown peaks appeared in the ^{1}H NMR spectrum after the reaction (Figure S7 in Supporting Information), suggesting the occurrence of side reactions (degradation of DMDL), although exact side reactions are unclear at this moment. For AAm, an insoluble polymer gel was generated (insoluble in *N*,*N*-dimethylformamide (DMF), tetrahydrofuran (THF), dichloromethane, and acetone).

We studied the copolymerization with VAc, which is a member of the family of LAM (Table 1, entry 10). VAc was still consumed faster than DMDL (Figure 6a). The VAc/

https://doi.org/10.1021/acs.macromol.4c01638
Macromolecules 2024, 57, 8983−8997

Table 3. Random Copolymerizations of DMDL with MMA and VAc at Varied Feed Monomer Compositions

entry	comonomer (M)	CTA	$[M]_0/[DMDL]_0/[CTA]_0/[AIBN]_0$[a] (equiv)	T (°C)	t (h)	conv.[b] (M/DMDL) (%/%)	overall conv.[c] (%)	M_n[d] ($M_{n,theo}$[e])	$Đ$[d]	F_{DMDL} (%)[f]
1	MMA	CDPA	90/10/1/0.2	70	24	97/29	90	11000 (9500)	1.31	3
2	MMA	CDPA	70/30/1/0.2	70	24	100/61	88	12000 (9700)	1.81	21
3	MMA	CDPA	50/50/1/0.2	70	24	100/52	76	13000 (8700)	2.01	34
4	MMA	CDPA	30/70/1/0.2	70	24	100/47	63	17000 (7600)	1.58	52
5	MMA	CDPA	10/90/1/0.2	70	24	100/40	46	19000 (6000)	1.68	78
6	VAc	ECP	90/10/1/0.2	70	24	94/66	91	5700 (8300)	1.36	7
7	VAc	ECP	70/30/1/0.2	70	24	100/68	90	5500 (8900)	1.32	23
8	VAc	ECP	50/50/1/0.2	70	24	100/60	80	5100 (8400)	1.23	38
9	VAc	ECP	30/70/1/0.2	70	24	100/73	81	4900 (9300)	1.30	63
10	VAc	ECP	10/90/1/0.2	70	24	100/53	58	4800 (7200)	1.33	83

[a]Solution polymerization in DMF (70 wt %) with 30 wt % of monomers in total. [b]Monomer conversions of comonomer (M) and DMDL determined with ^{1}H NMR. [c]Overall monomer conversion of the two monomers calculated according to (conversion of DMDL) × (initial fraction of DMDL) + (conversion of comonomer) × (initial fraction of comonomer). [d]PMMA-calibrated GPC values (DMF eluent). [e]Theoretical M_n calculated according to ($[monomers]_0/[CTA]_0$) × (monomer conversion) × (molecular weight of monomer) + (molecular weight of CTA). [f]Fraction of DMDL calculated from the monomer conversions (monomer consumption) of DMDL and comonomer.

DMDL system has r_{VAc} = 1.65 and r_{DMDL} = 0.29.[25] The product of r_{VAc} and r_{DMDL} (1.65 × 0.29 = 0.48) is closer to 1, suggesting that the monomer sequence is more random in the VAc/DMDL system than in the MMA/DMDL and BA/DMDL systems. Also, the r_{DMDL} value (0.29) is not nearly zero in the VAc system in contrast to the MMA and BA systems (nearly zero and 0.03), meaning that the DMDL terminal radical can react with DMDL to more extents in the VAc system for generating a consecutive DMDL−DMDL monomer unit sequence. The M_n value increased with an increase in the overall monomer conversion, and the $Đ$ value was low (1.13−1.23) up to an 80% overall monomer conversion (Figure 6b). Similarly, the copolymerization with VP, which is another family of LAM, yielded a low-dispersity copolymer with M_n = 3400, $Đ$ = 1.19, and F_{DMDL} = 36% for 24 h (Table 2, entry 11 and Figure 6c,d), although the polymerization was relatively slow (42% overall monomer conversion for 24 h).

For CTA, instead of ECP, we also used CDPA in the copolymerization of the two LAMs (VAc and VP). For the VAc/DMDL system, the use of CDPA (Table 1, entry 12 and Figure S8 in Supporting Information) resulted in a smaller molecular weight and a larger dispersity than the use of ECP, probably because the radical generated from CDPA is more stable than that from ECP and underwent propagation in a less efficient manner (and would tend to undergo radical−radical termination). Probably for the same reason, the use of CDPA in the VP/DMDL system also resulted in an inefficient polymerization, generating only oligomers (M_n < 1000) (Table 1, entry 13).

We also studied the MMA/DMDL and VAc/DMDL systems at varied DMDL feed monomer compositions (f_{DMDL}) of 10−90% at 70 °C for 24 h (Table 3 and Figures S9−S18 in Supporting Information). MMA and VAc were chosen as representative MAM and LAM, respectively. In the MMA/DMDL system, while the conversion of MMA was close to 100% (97−100%) at all studied f_{DMDL} values, that of DMDL ranged from 29 to 61% (Table 3, entries 1−5). The F_{DMDL} value increased from 3 to 78% with an increase in the f_{DMDL} value. The $Đ$ value (1.31, 2.01) was relatively large. In the VAc/DMDL system, the conversions of both VAc (94−100%) and DMDL (53−73%) were high, and the $Đ$ value (1.23−1.36) was relatively small at all studied f_{DMDL} values (Table 3, entries 6−10) because of the closer reactivities of DMDL and VAc. (The smaller $Đ$ value in the VAc/DMDL system would be ascribed to the actual narrower molecular weight distribution but might also be partly ascribed to a possibly less variation in the monomer composition (less variation in monomer composition-dependent hydrodynamic volume) among the generated polymer chains.) The F_{DMDL} value increased from 7 to 83% with an increase in the f_{DMDL} value. Figure 7 shows the plot of F_{DMDL} vs f_{DMDL} in the MMA/DMDL and VAc/DMDL systems (Table 3), showing a nearly linear relation of F_{DMDL} to f_{DMDL} for both systems.

Block Polymerizations. To obtain a well-defined block copolymer, monomer addition order is crucial in RAFT polymerization.[46] In the RAFT process, from an intermediate radical, a more stabilized propagating radical is fragmented. Hence, the first monomer should be chosen to generate a more stabilized radical in comparison to the second monomer. We synthesized block copolymers using VAc and VP for the first block and DMDL for the second block (Figure 8a and 8b and Table 4, entries 1 and 2). The propagating radicals from the PVAc and PVP macro-chain-transfer agent (macro-CTA) are more stable than that of PDMDL and efficiently underwent fragmentation from the intermediate radical, resulting in chain extension, where PVAc and PVP are poly(vinyl acetate) and poly(vinylpyrrolidone), respectively. The M_n value increased from 6700 to 13000 for the VAc/DMDL system and from 6800 to 9000 for the VP/DMDL system (Table 4, entries 1 and 2). The GPC chromatograms (Figure 8a,b) smoothly shifted to the high molecular weight side, suggesting that a large amount of the macro-CTA extended. We also attempted

https://doi.org/10.1021/acs.macromol.4c01638
Macromolecules 2024, 57, 8983−8997

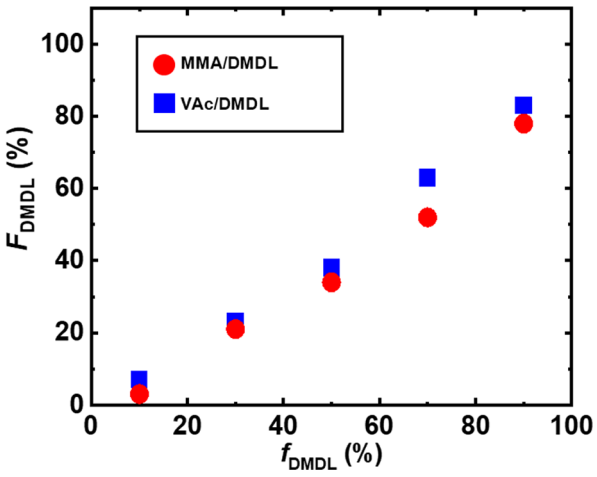

Figure 7. Plot of DMDL polymer composition (F_{DMDL}) vs DMDL feed monomer composition (f_{DMDL}) for the MMA/DMDL/CDPA/AIBN (Table 3, entries 1−5) and VAc/DMDL/ECP/AIBN (Table 3, entries 6−10) systems at varied f_{DMDL} values (70 °C): $[comonomer]_0$ = 90−10 equiv; $[DMDL]_0$ = 90−10 equiv; $[CDPA\ or\ ECP]_0$ = 1 equiv; $[AIBN]_0$ = 0.2 equiv. The symbols are indicated in the figure. The F_{DMDL} value was calculated from the monomer conversions (monomer consumption) of DMDL and comonomer (MMA or VAc).

to use MMA and NIPAm (MAMs) instead of VAc and VP (LAMs) for the first block. However, the propagating radical from macro-CTA was too stable to efficiently initiate the polymerization of DMDL, resulting in inefficient block polymerization. In order to obtain a block copolymer containing a MAM comonomer, we used a BA/DMDL random copolymer (PBA-*r*-PDMDL) as macro-CTA (first block segment) to extend DMDL (second block segment) because the random copolymer macro-CTA would contain DMDL as a terminal monomer unit to a certain extent, which would facilitate the propagation (the addition of the macro-CTA propagating radical) to DMDL to form the second block PDMDL segment. The GPC chromatogram (Figure 8c) slightly shifted to the high molecular weight side, and the M_n value increased from 10000 to 12000 (Table 4, entry 3). The only slight shift would suggest a limitation in the use of the MAM monomer in macro-CTA in the present system.

We also studied a chain extension from a PDMDL macro-CTA to extend DMDL. The GPC chromatogram (Figure 8d) showed that a majority of the PDMDL macro-CTA extended to the high molecular weight side and the M_n value increased from 3800 to 4500 (Table 4, entry 4), confirming that the DMDL terminal unit in the macro-CTA can efficiently initiate the polymerization of DMDL.

We carried out peak resolution of the GPC chromatograms (Figure S19 in Supporting Information) and ^{1}H NMR analysis (Figure S20 in Supporting Information) to estimate how much of the macro-CTA extended. The results showed that the block efficiency was relatively high at least for the PVAc, PVP, and PDMDL macro-CTA systems (Table 4, entries 1, 2, and 4, and Figure 8).

Degradation of Homopolymers and Random Copolymers of DMDL. We studied the base (NaOH)-assisted degradation of homopolymers and random copolymers synthesized via RAFT polymerization (Table 5). The syntheses of these polymers are given in Table S1 and Supporting Information.

To study the degradation, we dissolved a polymer (8 wt %) in dimethyl sulfoxide (DMSO) (92 wt %), and to this solution (4.8 g), we added an aqueous NaOH solution (0.5 g for homopolymers and 0.2 g for random copolymers) (NaOH/water = 29/71 wt %) and then stirred the mixture at room temperature for 24 h (Table 5). We used DMSO as a solvent because DMSO can dissolve both hydrophobic and hydrophilic polymers. We used an excess of NaOH (1.1−2.7 equiv

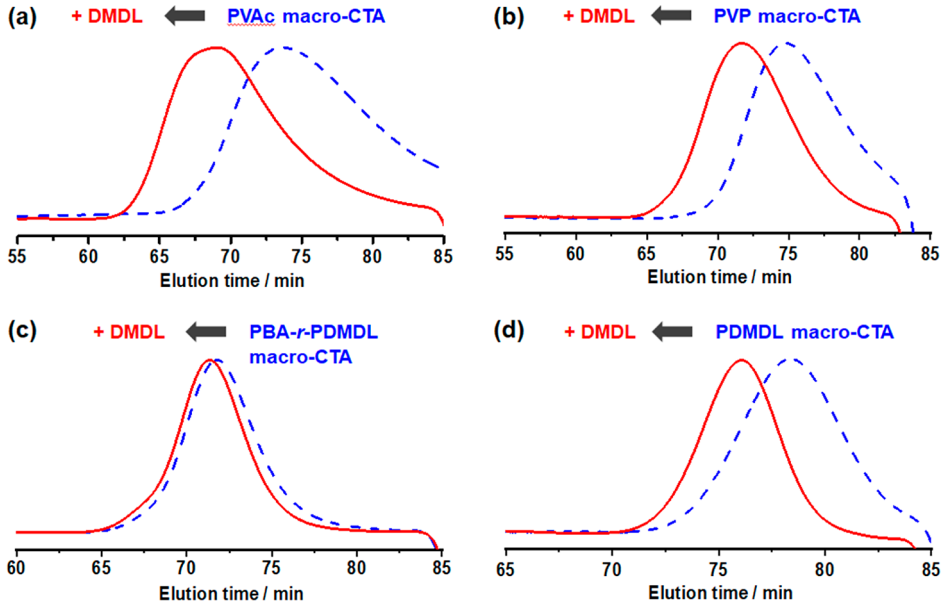

Figure 8. GPC chromatograms in block polymerizations of (a) PVAc macro-CTA (first block) with DMDL (second block), (b) PVP macro-CTA (first block) with DMDL (second block), and (c) PBA-*r*-PDMDL macro-CTA (first block) with DMDL (second block) and (d) chain extension of PDMDL macro-CTA (first block) with DMDL (second block). The blue dashed lines show macro-CTA, and the red solid lines show (a−c) block copolymers and (d) chain-extended PDMDL homopolymer. The reaction conditions for (a−d) are given in Table 4, entries 1−4, respectively.

https://doi.org/10.1021/acs.macromol.4c01638
Macromolecules 2024, 57, 8983−8997

Table 4. Block Polymerizations (Entries 1−3) and Chain Extension (Entry 4) Using DMDL

entry	first monomer	second monomer	CTA[a]	$[monomer]_0/[CTA]_0/[AIBN]_0$[b] (equiv)	T (°C)	t (h)	conv.[c] (%)	M_n[d] ($M_{n,theo}$[e])	$Đ$[d]
1	VAc		ECP	100/1/0.2	70	24	98	6700 (8700)	1.35
		DMDL	PVAc−X	200/1/0.2	70	24	43	13,000 (20000)	1.62
2	VP		ECP	100/1/0.2	70	24	33	6800 (3900)	1.61
		DMDL	PVP−X	100/1/0.2	70	24	56	9000 (11000)	1.31
3	BA/DMDL[f]		CDPA	50/50/1/0.2	70	24	100/87	10000 (12400)	1.18
		DMDL	PBA-*r*-PDMDL−X	100/1/0.2	70	24	27	12000 (15900)	1.19
4	DMDL		ECP	50/1/0.2	70	24	65	3800 (4400)	1.09
		DMDL	PDMDL−X	100/1/0.2	70	24	35	4500 (8900)	1.08

[a]X = S(C = S)OC2H5. [b]Solution polymerization in DMF (70 wt %) with 30 wt % of monomers in total. [c]Monomer conversion determined with ^{1}H NMR. [d]PMMA-calibrated GPC values (DMF eluent). The M_n and $Đ$ values for the first block (macro-CTA) are those after purification. The M_n and $Đ$ values for the block copolymers (entries 1−3) and chain-extended polymer (entry 4) are those before purification. [e]Theoretical M_n calculated according to ($[monomer]_0/[CTA]_0$) × (monomer conversion) × (molecular weight of monomer) + (molecular weight of CTA) for the first block and ($[DMDL]_0/[macro\text{-}CTA]_0$) × (DMDL conversion) × (molecular weight of DMDL) + (theoretical molecular weight of macro-CTA) for the second block. [f]Random copolymerization.

Table 5. Degradation of Homopolymers and Random (Gradient) Copolymers of DMDL

		before degradation				after degradation for 24 h
entry	polymer[a]	M_n[b]	$Đ$[b]	M_p[b,c]	F_{DMDL}[d] (%)	M_p[b,c]
1	PDMDL (RAFT polymerization using ECP)	9600	1.28	12000	100	
2	PDMDL (conventional radical polymerization)	14000	1.41	18000	100	
3	PMMA-*r*-PDMDL	22000	1.81	41000	18	13000
4	PNIPAm-*r*-PDMDL	17000	1.27	22000	43	6900
5	PVAc-*r*-PDMDL	6700	1.27	7500	36	80000
6	PVP-*r*-PDMDL	4400	1.23	4700	23	3100

[a]The synthetic conditions of the polymers are given in Table S1 in Supporting Information. [b]PMMA-calibrated GPC values using DMF eluent. [c]GPC peak-top molecular weight. [d]Fraction of DMDL in the copolymer (after purification) determined by ^{1}H NMR.

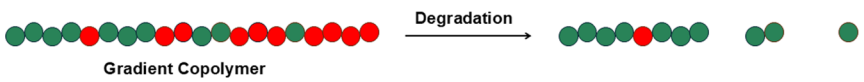

Figure 9. Illustration of degradation of random (gradient) copolymer. The backbone cleavage occurs only at a point where two (or more) DMDL monomer units are successively sequenced and will not occur at a point where only one DMDL unit is present along the chain.

to the DMDL unit in the polymer) to ensure complete degradation.

We first studied the degradation of the PDMDL homopolymers synthesized via conventional radical polymerization and RAFT polymerization (Table 5, entries 1 and 2). In both cases, the polymer rapidly degraded, showing nearly 100% degradation after 1 h from the addition of the NaOH solution (Figure S21 in Supporting Information). The result suggests that the use of a RAFT agent has virtually no effect on the ability of PDMDL to degrade in this degradation condition.

Figure 9 illustrates how random (gradient) copolymers can degrade. As mentioned above, RAFT random copolymerization yields gradient copolymer chains with a sequential change from a comonomer-rich sequence (initial segment of the chain) to a DMDL-rich sequence (end segment of the chain). Thus, degradation of the gradient copolymer would generate oligomers with varied sizes from relatively large sizes (initial segment of the polymer) to relatively small sizes (end segment of the polymer).

For the random (gradient) copolymers, Figure 10 shows the GPC chromatograms and the plot of the GPC peak-top molecular weight (M_p) value vs the degradation time. We used the M_p value instead of the M_n value because the GPC chromatogram had a significant tailing to the low molecular weight side after degradation (because of the formation of oligomers with small sizes) and it was difficult to set a baseline for determining the M_n value. For the MMA/DMDL copolymer (Table 5, entry 3, and Figure 10a), the M_p value decayed from 41000 (original) to 16000 after 4 h degradation and 13000 after 24 h degradation. As mentioned, backbone cleavage can occur when two units of DMDL are successively present side by side. Hence, the comonomer-rich (MMA-rich) segment tended to be retained during the degradation, and the DMDL-rich sequence tended to significantly degrade. Thus, the observed M_p value would mainly correspond to oligomers with relatively large sizes originated from the MMA-rich segment. In general, comparing among the same (methacrylate) family of comonomers, the degradability might depend on the hydrophilicity of the comonomer. Hydrophilic copolymers are more soluble in water (hence they can more readily contact NaOH) than hydrophobic copolymers and hence might degrade faster. Nevertheless, the MMA/DMDL copolymer degraded relatively rapidly despite its hydrophobicity, suggesting that hydrophilic methacrylate copolymers may degrade even faster, but both hydrophobic and hydrophilic methacrylate copolymers may degrade sufficiently fast for the methacrylate/DMDL copolymers.

The NIPAm/DMDL copolymer (Table 5, entry 4, and Figure 10b) degraded similarly, and the M_p value decayed from 22000 (original) to 11000 after 4 h degradation and 6900 after 24 h degradation. The VP/DMDL copolymer (Table 5, entry

https://doi.org/10.1021/acs.macromol.4c01638
Macromolecules 2024, 57, 8983−8997

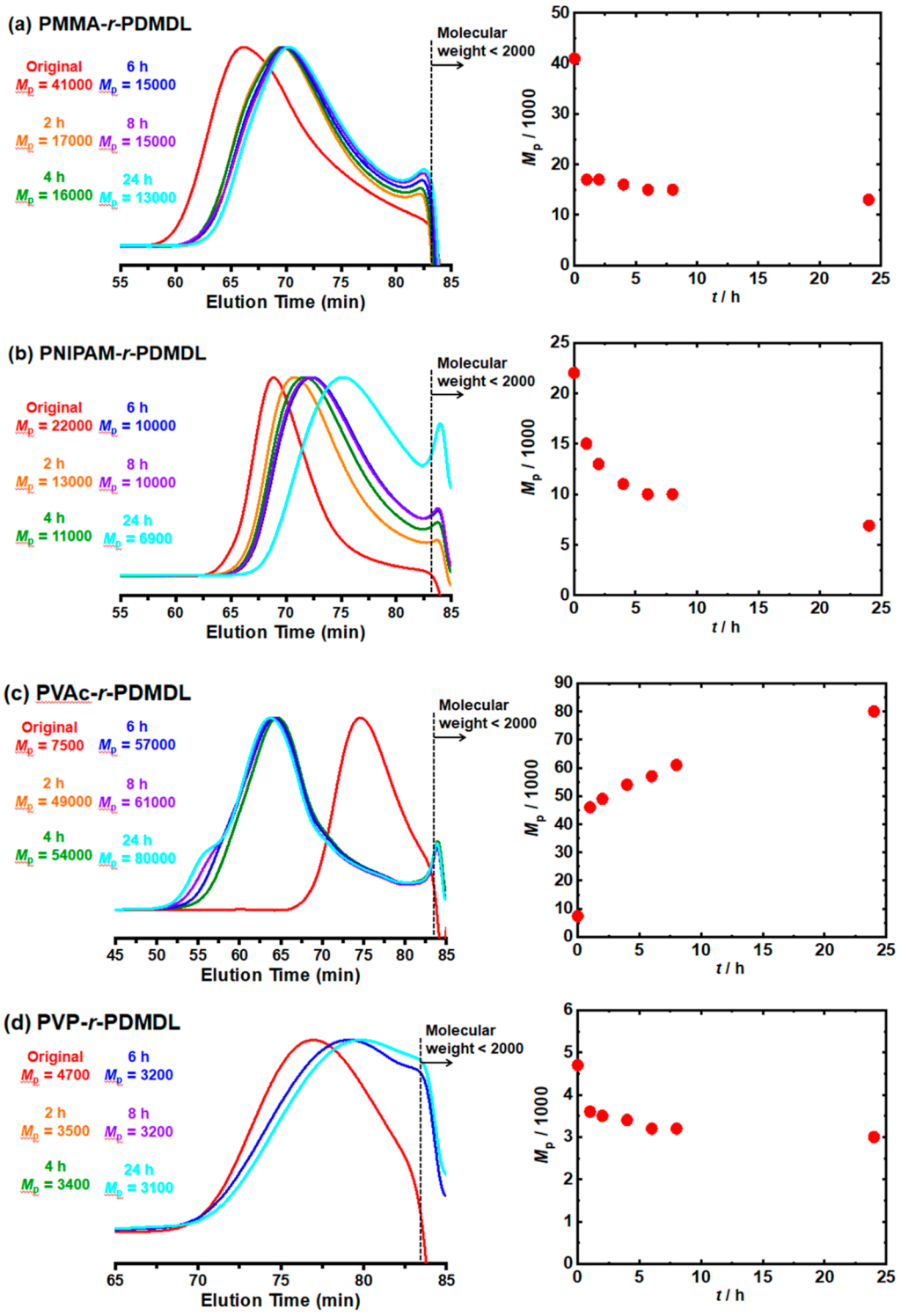

Figure 10. GPC chromatograms and plots of GPC peak-top molecular weight (M_p) vs degradation time for base-assisted degradation of (a) MMA/DMDL, (b) NIPAm/DMDL, (c) VAc/DMDL, and (d) VP/DMDL random (gradient) copolymers. A solution (4.8 g) of a polymer (8 wt %) and DMSO (92 wt %) was mixed with an aqueous NaOH solution (0.2 g) (NaOH/water = 29/71 wt %).

6, and Figure 10d) degraded to a lesser extent. The M_p value decayed from 4700 (original) to 3400 after 4 h of degradation and 3100 after 4 h of degradation. The lesser extent of the degradation is partly ascribed to the relatively small F_{DMDL} (=23%) value of the VP/DMDL copolymer, which is however still a similar value to that (=18%) of the MMA/DMDL copolymer that more significantly degraded (Table 5, entry 3, and Figure 10a). The exact reason for the lower degradation of the VP/DMDL copolymer is not clear at this moment.

For the VAc/DMDL copolymer (Table 5, entry 5, and Figure 10c), the M_p value apparently increased from 7500 (original) to 54000 after 4 h degradation and 80000 after 24 h degradation. The VAc units in the copolymer underwent hydrolysis under basic (high pH) conditions, generating hydroxyl groups on the polymer chain. The generated hydroxyl

https://doi.org/10.1021/acs.macromol.4c01638
Macromolecules 2024, 57, 8983−8997

Table 6. Random Copolymerizations of DMDL with VP or BA

						before purification			after purification		
entry	comonomer (M)	CTA	$[M]_0/[DMDL]_0/[CTA]_0/[AIBN]_0$[a] (equiv)	T (°C)	t (h)	conv.[b] (M/DMDL) (%/%)	M_n[c] ($M_{n,theo}$[d])	$Đ$[c]	M_n[c,f]	$Đ$[c]	F_{DMDL} (%)[e,f]
1	VP	ECP	70/30/1/0.2	70	24	74/100	10000 (9800)	1.28	9800	1.24	12
2	VP	ECP	30/70/1/0.2	70	24	81/70	10000 (9200)	1.30	10000	1.23	27
C1	BA	CDPA	70/30/1/0.2	70	24	100/79	10000 (12000)	1.42	9600	1.35	24

[a]Solution polymerization in DMF (70 wt %) with 30 wt % of monomers in total. [b]Monomer conversions of comonomer (M) and DMDL determined with ^{1}H NMR. [c]PMMA-calibrated GPC values (DMF eluent). [d]Theoretical M_n calculated according to ($[monomers]_0/[CTA]_0$) × (monomer conversion) × (molecular weight of monomer) + (molecular weight of CTA). [e]Fraction of DMDL determined with ^{1}H NMR. [f]The F_{DMDL} values after purification (determined with ^{1}H NMR) were somewhat smaller than those before purification (calculated from the monomer conversions (monomer consumption) of DMDL and comonomer), probably because DMDL-richer polymers tended to dissolve in the reprecipitation (purification) solvent (1/1 hexane/diethyl ether for entries 1 and 2 and 9/1 methanol/water for entry C1) and be removed from the purified polymers. The M_n values after purification (reprecipitation) were slightly smaller than those before purification, also probably because DMDL-richer polymers tended to be removed.

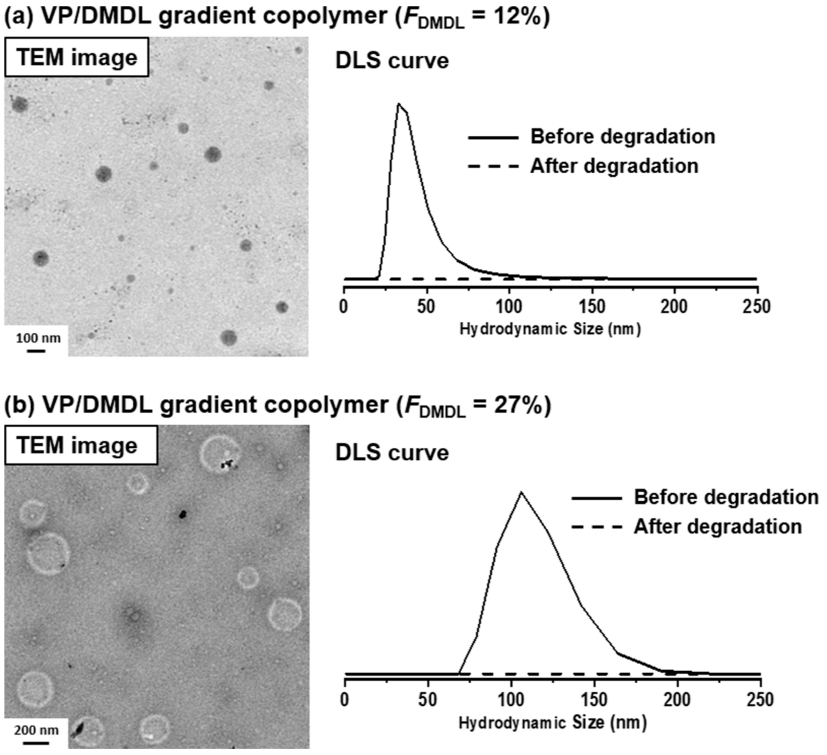

Figure 11. TEM images and DLS curves of self-assemblies of VP/DMDL gradient copolymers with (a) M_n = 9800, $Đ$ = 1.24, and F_{DMDL} = 12% (Table 6, entry 1) and (b) M_n = 10,000, $Đ$ = 1.23, and F_{DMDL} = 27% (Table 6, entry 2). In the DLS curves, the solid lines show the assemblies before the addition of the aqueous NaOH solution, and the dashed lines show no assemblies retained after the addition of the aqueous NaOH solution.

groups seemed to form strong hydrogen bonds among the hydroxyl groups, which would result in intermolecular association of the degraded oligomers. The backbone degradation of the original copolymer would occur, but the intermolecular association of the degraded oligomers would give the apparent increase in the M_p value.

As observed for the VAc copolymer (Figure 10c and Table 5, entry 5), hydrolysis may significantly occur for the acrylate copolymer at the side chain. Hence, we did not study the degradation of the acrylate copolymer. Hydrolysis may also occur for the methacrylate copolymer at the side chain particularly at an elevated temperature, although a methacrylate unit is much less hydrolyzable than an acrylate unit,[59] and we also studied the degradation at room temperature. To study possible hydrolysis, we analyzed the degraded oligomer from PMMA-*r*-PDMDL using ^{1}H NMR (Figure S22 in Supporting Information). The result showed no significant hydrolysis of the side chain of the MMA monomer unit, suggesting that the observed decrease in the M_n value (Figure 10a and Table 5, entry 3) for the MMA/DMDL copolymer was mainly ascribed to the cleavage of the DMDL monomer units in the backbone chain. The side chains in the NIPAM and VP units are amides, which are even less hydrolyzable than the ester in the MMA unit. Thus, the increase in the M_p value (Figure 10c) would be specific to the VAc/DMDL copolymer due to the readily hydrolyzable side group in the VAc unit.

https://doi.org/10.1021/acs.macromol.4c01638
Macromolecules 2024, 57, 8983−8997

We also studied the degradation of a copolymer under acidic conditions. We dissolved PNIPAm-*r*-PDMDL (Table 5, entry 4) (M_n = 17,000) (10 wt %) in a mixed solvent of DMSO (79.5 wt %) and water (1.5 wt %) to which trifluoroacetic acid (TFA) (9 wt %) was added. The mixture was stirred for 3 days at 80 °C. The M_p value decreased from 22000 (before the TFA treatment) to 6700 (after the TFA treatment) (Figure S23 in Supporting Information), demonstrating the acid-catalyzed degradation. A possible mechanism of the acid-catalyzed degradation was previously discussed,[25] but the exact mechanism is still unclear at this moment.

Application for Creation of Degradable Self-Assemblies. An advantage of RAFT random copolymerization of DMDL is the generation of gradient copolymers owing to the different reactivities of DMDL and comonomers. Such gradient copolymers with a DMDL-rich segment and a comonomer-rich segment may offer similar properties to those of block copolymers.[39,40] The synthesis of gradient copolymers requires only a single polymerization (single step), which is advantageous over the synthesis of block copolymers, which requires two polymerizations (two steps). In the present work, we synthesized VP/DMDL gradient copolymers. The polymers are amphiphilic, and we used them to generate self-assemblies (micelles and vesicles)[30,47−58] in water.

We carried out random copolymerizations of VP and DMDL via RAFT polymerization and obtained gradient copolymers with two different F_{DMDL} values (=12% and 27%) (Table 6). The obtained gradient copolymer (1 wt %) was dissolved in THF (9 wt %), which was dropped in water (90 wt %) to form a self-assembly. A droplet of the mixture was cast on a copper grid, dried, and analyzed using transmission electron microscopy (TEM). A VP/DMDL gradient copolymer with M_n = 9800, $Đ$ = 1.24, and F_{DMDL} = 12% (Table 6, entry 1) formed a micelle, as the TEM image shows (Figures 11a and S24a in Supporting Information). The mixture was also 10 times diluted with water and analyzed with dynamic light scattering (DLS). The hydrodynamic size (DLS peak top) of the assembly in water was 29 nm (Figure 11a). A VP/DMDL gradient with M_n = 10,000, $Đ$ = 1.23, and F_{DMDL} = 27% (Table 6, entry 2) formed a vesicle, as observed with TEM, although the exact internal structure of the vesicle (entire cavity or possible inclusion of smaller assemblies in the vesicle) is unclear from the obtained TEM image. The hydrodynamic size (DLS peak top) of the assembly in water was 176 nm (Figures 11b and S24b in Supporting Information). As a comparison experiment, we also synthesized a BA/DMDL gradient copolymer with M_n = 9600, $Đ$ = 1.35, and F_{DMDL} = 24% (Table 6, entry C1). Because both BA and DMDL are hydrophobic, the obtained gradient copolymer was hydrophobic. The polymer did not form a nanostructured self-assembly in water but precipitated onto a wall of a glass vial (Figure S25 in Supporting Information), confirming the need for a combination of a hydrophilic comonomer (VP) with DMDL to generate self-assemblies.

We degraded the obtained self-assemblies (micelles and vesicles) under basic conditions (Figure 11). To the above-obtained mixture (1.0 g) of assemblies (1 wt %), THF (9 wt %), and water (90 wt %), 0.2 g of aqueous NaOH solution (NaOH/water = 20/80 wt %) was added. The solution was stirred at room temperature for 24 h. DLS analysis showed no assemblies retained after the NaOH treatment for both the micelle (Figure 11a (dashed line)) and the vesicle (Figure 11b (dotted line)), demonstrating the degradation of the assemblies under the basic conditions. To confirm that the VP units did not degrade, we treated a PVP homopolymer in the same degradation (aqueous NaOH) solution for 24 h. No change was observed in the GPC chromatograms before and after the treatment (Figure S26 in Supporting Information), suggesting that the VP units did not degrade by the NaOH treatment and that the observed degradation of the self-assemblies was ascribed to the degradation of the DMDL-containing sequence.

As comparison experiments, we also dispersed PDMDL homopolymer, PVP-*r*-PDMDL, and PVP-*b*-PDMDL in neutral water and observed no degradation after 24 h of stirring (Figure S27 in Supporting Information), suggesting that the DMDL units in the polymers are stable in water at a neutral pH for 24 h.

CONCLUSIONS

Using RAFT polymerization, we synthesized homopolymers, random (gradient) copolymers, and block copolymers of DMDL with relatively low dispersities. Various hydrophobic and hydrophilic monomers, including methacrylates, acrylates, AAms, VAc, and VP, were amenable to copolymerization. Because the studied comonomers were more reactive than DMDL, the random copolymerization tended to yield gradient copolymers, which are attainable via RAFT polymerization (living radical polymerization) but not via conventional radical polymerization. The obtained random (gradient) copolymers degraded under basic conditions in relatively short times. As an application, gradient copolymers with hydrophobic DMDL-rich segments and hydrophilic VP-rich segments were used to generate degradable micelles and vesicles, whose degradation was also demonstrated. The synthesis of gradient copolymers requires only a single-step polymerization, which is advantageous over the synthesis of block copolymers, which requires two polymerizations.

ASSOCIATED CONTENT

Supporting Information

The Supporting Information is available free of charge at https://pubs.acs.org/doi/10.1021/acs.macromol.4c01638.

Experimental section, polymerization data, degradation data, and self-assembly data, including polymerization data and ^{1}H NMR spectra, polymerization behaviors, GPC chromatograms, TEM images, and a photograph (PDF)

AUTHOR INFORMATION

Corresponding Author

Atsushi Goto − *School of Chemistry, Chemical Engineering and Biotechnology, Nanyang Technological University, Singapore 637459, Singapore;* orcid.org/0000-0001-7643-3169; Email: agoto@ntu.edu.sg

Authors

Tze Kwang Gerald Er − *School of Chemistry, Chemical Engineering and Biotechnology, Nanyang Technological University, Singapore 637459, Singapore;* orcid.org/0000-0002-7268-6553

Xuan Yong Haydon Lim − *School of Chemistry, Chemical Engineering and Biotechnology, Nanyang Technological University, Singapore 637459, Singapore*

https://doi.org/10.1021/acs.macromol.4c01638
Macromolecules 2024, 57, 8983−8997

Xin Yi Oh − *School of Chemistry, Chemical Engineering and Biotechnology, Nanyang Technological University, Singapore 637459, Singapore;* Present Address: Institute of Sustainability for Chemicals, Energy and Environment (ISCE2), Agency for Science, Technology and Research (A*STAR), 1 Pesek Road, Jurong Island, Singapore 627833, Singapore; orcid.org/0000-0003-1944-2362

Complete contact information is available at: https://pubs.acs.org/10.1021/acs.macromol.4c01638

Author Contributions

The manuscript was written through contributions of all authors. All authors have given approval to the final version of the manuscript.

Notes

The authors declare no competing financial interest.

■ ACKNOWLEDGMENTS

This work was supported by RIE2025 Manufacturing, Trade, and Connectivity (MTC) Programmatic Fund of Agency for Science, Technology and Research (A*STAR) (grant number: M22K9b0049).

■ REFERENCES

(1) Lefay, C.; Guillaneuf, Y. Recyclable/degradable materials via the insertion of labile/cleavable bonds using a comonomer approach. *Prog. Polym. Sci.* **2023**, *147*, 101764.
(2) Kim, M. S.; Chang, H.; Zheng, L.; Yan, Q.; Pfleger, B. F.; Klier, J.; Nelson, K.; Majumder, E. L. W.; Huber, G. W. A Review of Biodegradable Plastics: Chemistry, Applications, Properties, and Future Research Needs. *Chem. Rev.* **2023**, *123*, 9915−9939.
(3) Martinez, M. R.; Matyjaszewski, K. Degradable and Recyclable Polymers by Reversible Deactivation Radical Polymerization. *CCS Chem.* **2022**, *4*, 2176−2211.
(4) Zhang, S.; Li, R.; An, Z. Degradable Block Copolymer Nanoparticles Synthesized by Polymerization-Induced Self-Assembly. *Angew. Chem.* **2024**, *136*, No. e202315849.
(5) Kamaly, N.; Yameen, B.; Wu, J.; Farokhzad, O. C. Degradable Controlled-Release Polymers and Polymeric Nanoparticles: Mechanisms of Controlling Drug Release. *Chem. Rev.* **2016**, *116*, 2602−2663.
(6) Amobonye, A.; Bhagwat, P.; Singh, S.; Pillai, S. Plastic biodegradation: Frontline microbes and their enzymes. *Sci. Total Environ.* **2021**, *759*, 143536.
(7) Shi, C.; Quinn, E. C.; Diment, W. T.; Chen, E. Y.-X. Recyclable and (Bio)degradable Polyesters in a Circular Plastics Economy. *Chem. Rev.* **2024**, *124*, 4393−4478.
(8) Wang, Y.; van Putten, R.-J.; Tietema, A.; Parsons, J. R.; Gruter, G.-J. M. Polyester biodegradability: importance and potential for optimisation. *Green Chem.* **2024**, *26*, 3698−3716.
(9) Wang, L.; Li, Y.; Yang, J.; Wu, Q.; Liang, S.; Liu, Z. Poly(Propylene Carbonate)-Based Biodegradable and Environment-Friendly Materials for Biomedical Applications. *Int. J. Mol. Sci.* **2024**, *25*, 2938.
(10) Dirauf, M.; Muljajew, I.; Weber, C.; Schubert, U. S. Recent advances in degradable synthetic polymers for biomedical applications- Beyond polyesters. *Prog. Polym. Sci.* **2022**, *129*, 101547.
(11) Bailey, W. J.; Ni, Z.; Wu, S. R. Free Radical Ring-Opening Polymerization of 4,7-Dimethyl-2-Methylene-1,3-Dioxepane and 5,6-Benzo-2-Methylene-1,3-Dioxepane. *Macromolecules* **1982**, *15*, 711−714.
(12) Tardy, A.; Nicolas, J.; Gigmes, D.; Lefay, C.; Guillaneuf, Y. Radical Ring-Opening Polymerization: Scope, Limitations, and Application to (Bio)Degradable Materials. *Chem. Rev.* **2017**, *117*, 1319−1406.
(13) Hedir, G. G.; Arno, M. C.; Langlais, M.; Husband, J. T.; O'Reilly, R. K. O.; Dove, A. P. Poly(oligo(ethylene glycol) vinyl acetate)s: A Versatile Class of Thermoresponsive and Biocompatible Polymers. *Angew. Chem.* **2017**, *129*, 9306−9310.
(14) Pesenti, T.; Nicolas, J. 100th Anniversary of Macromolecular Science Viewpoint: Degradable Polymers from Radical Ring-Opening Polymerization: Latest Advances, New Directions, and Ongoing Challenges. *ACS Macro Lett.* **2020**, *9*, 1812−1835.
(15) Lena, J.-B.; Jackson, A. W.; Chennamaneni, L. R.; Wong, C. T.; Lim, F.; Andriani, Y.; Thoniyot, P.; van Herk, A. M. Degradable Poly(alkyl acrylates) with Uniform Insertion of Ester Bonds, Comparing Batch and Semibatch Copolymerizations. *Macromolecules* **2020**, *53*, 3994−4011.
(16) Folini, J.; Wurad, W.; Mehner, F.; Meier, W.; Gaitzsch, J. Updating Radical Ring-Opening Polymerisation of Cyclic Ketene Acetals from Synthesis to Degradation. *Eur. Polym. J.* **2020**, *134*, 109851.
(17) Jackson, A. W. Reversible-deactivation radical polymerization of cyclic ketene acetals. *Polym. Chem.* **2020**, *11* (21), 3525−3545.
(18) Zhu, C.; Nicolas, J. Bio)degradable and Biocompatible Nano-Objects from Polymerization-Induced and Crystallization-Driven Self Assembly. *Biomacromolecules* **2022**, *23*, 3043−3080.
(19) Deng, Y.; Mehner, F.; Gaitzsch, J. Current Standing on Radical Ring-Opening Polymerizations of Cyclic Ketene Acetals as Homopolymers and Copolymers with one another. *Macromol. Rapid Commun.* **2023**, *44*, 2200941.
(20) Carter, M. C. D.; Hejl, A.; Woodfin, S.; Einsla, B.; Janco, M.; DeFelippis, J.; Cooper, R. J.; Even, R. C. Backbone-Degradable Vinyl Acetate Latex: Coatings for Single-Use Paper Products. *ACS Macro Lett.* **2021**, *10* (5), 591−597.
(21) Carlotti, M.; Tricinci, O.; Mattoli, V. Novel, High-Resolution, Subtractive Photoresist Formulations for 3D Direct Laser Writing Based on Cyclic Ketene Acetals. *Adv. Mater. Technol.* **2022**, *7* (9), 2101590.
(22) Gil, N.; Thomas, C.; Mhanna, R.; Mauriello, J.; Maury, R.; Leuschel, B.; Malval, J. P.; Clément, J.; Gigmes, D.; Lefay, C.; et al. Thionolactone as a Resin Additive to Prepare (Bio) degradable 3D Objects via VAT Photopolymerization. *Angew. Chem., Int. Ed.* **2022**, *61* (18), No. e202117700.
(23) Zhang, Y.; Chu, D.; Zheng, M.; Kissel, T.; Agarwal, S. Biocompatible and degradable poly (2-hydroxyethyl methacrylate) based polymers for biomedical applications. *Polym. Chem.* **2012**, *3* (10), 2752−2759.
(24) Maji, S.; Mitschang, F.; Chen, L.; Jin, Q.; Wang, Y.; Agarwal, S. Functional Poly (Dimethyl Aminoethyl Methacrylate) by Combination of Radical Ring-Opening Polymerization and Click Chemistry for Biomedical Applications. *Macromol. Chem. Phys.* **2012**, *213* (16), 1643−1654.
(25) Oh, X. Y.; Ge, Y.; Goto, A. Synthesis of degradable and chemically recyclable polymers using 4,4-disubstituted five-membered cyclic ketene hemiacetal ester (CKHE) monomers. *Chem. Sci.* **2021**, *12* (40), 13546−13556.
(26) Chiefari, J.; Chong, Y. K.; Ercole, F.; Krstina, J.; Jeffery, J.; Le, T. P. T.; Mayadunne, R. T. A.; Meijs, G. F.; Moad, C. L.; Moad, G.; Rizzardo, E.; Thang, S. H. Living Free-Radical Polymerization by Reversible Addition−Fragmentation Chain Transfer: The RAFT Process. *Macromolecules* **1998**, *31* (16), 5559−5562.
(27) Moad, G.; Rizzardo, E.; Thang, S. H. Living radical polymerization by the RAFT process a third update. *Aust. J. Chem.* **2012**, *65* (8), 985−1076.
(28) Moad, G.; Rizzardo, E.; Thang, S. H. RAFT Polymerization and Some of its Applications. *Chem.—Asian J.* **2013**, *8*, 1634−1644.
(29) Perrier, S. 50th Anniversary Perspective: RAFT Polymerization—A User Guide. *Macromolecules* **2017**, *50* (19), 7433−7447.
(30) Wan, J.; Fan, B.; Thang, S. H. RAFT-mediated Polymerization-Induced Self-Assembly (RAFT-PISA): Current Status and Future Directions. *Chem. Sci.* **2022**, *13*, 4192−4224.

(31) Parkatzidis, K.; Wang, H. S.; Truong, N. P.; Anastasaki, A. Recent Developments and Future Challenges in Controlled Radical Polymerization: A 2020 Update. *Chem.* **2020**, *6*, 1575−1588.
(32) Corrigan, N.; Jung, K.; Moad, G.; Hawker, C. J.; Matyjaszewski, K.; Boyer, C. Reversible-deactivation radical polymerization (Controlled/living radical polymerization): From discovery to materials design and applications. *Prog. Polym. Sci.* **2020**, *111*, 101311.
(33) Wu, C.; Corrigan, N.; Lim, C.-H.; Liu, W.; Miyake, G.; Boyer, C. Rational Design of Photocatalysts for Controlled Polymerization: Effect of Structures on Photocatalytic Activities. *Chem. Rev.* **2022**, *122*, 5476−5518.
(34) Aydogan, C.; Yilmaz, G.; Shegiwal, A.; Haddleton, D. M.; Yagci, Y. Photoinduced Controlled/Living Polymerizations. *Angew. Chem., Int. Ed.* **2022**, *61*, No. e202117377.
(35) Truong, N. P.; Jones, G. R.; Bradford, K. G. E.; Konkolewicz, D.; Anastasaki, A. A comparison of RAFT and ATRP methods for controlled radical polymerization. *Nat. Rev.* **2021**, *5*, 859−869.
(36) Lee, Y.; Boyer, C.; Kwon, M. S. Photocontrolled RAFT Polymerization: Past, PResent, and Future. *Chem. Soc. Rev.* **2023**, *52*, 3035−3097.
(37) Goto, A.; Fukuda, T. Kinetics of Living Radical Polymerization. *Prog. Polym. Sci.* **2004**, *29*, 329−385.
(38) Barner-Kowollik, C.; Buback, M.; Charleux, B.; Coote, M. L.; Drache, M.; Fukuda, T.; Goto, A.; Klumperman, B.; Lowe, A. B.; Mcleary, J. B.; Moad, G.; Monteiro, M. J.; Sanderson, R. D.; Tonge, M. P.; Vana, P. Mechanism and kinetics of dithiobenzoate-mediated RAFT polymerization. I. The current situation. *J. Polym. Sci., Part A: Polym. Chem.* **2006**, *44*, 5809−5831.
(39) Zaremski, M. Y.; Kalugin, D. I.; Golubev, V. B. Gradient copolymers: Synthesis, structure, and properties. *Polymer science. Series A, Chemistry, physics* **2009**, *51* (1), 103−122.
(40) Lutz, J.-F.; Pakula, T.; Matyjaszewski, K. *Synthesis and Properties of Copolymers with Tailored Sequence Distribution by Controlled/Living Radical Polymerization*; ACS Symposium Series; American Chemical Society: Washington, DC, 2003; Vol. *854*, pp 268−282.
(41) Steube, M.; Johann, T.; Barent, R. D.; Muller, A. H. E.; Frey, H. Rational design of tapered multiblock copolymers for thermoplastic elastomers. *Prog. Polym. Sci.* **2022**, *124*, 101488.
(42) Van Hook, J. P.; Tobolsky, A. V. The thermal Decomposition of 2,2'-Azo-bis-isobutyronitrile. *J. Am. Chem. Soc.* **1958**, *80*, 779−782.
(43) Buback, M.; Huckestein, B.; Kuchta, F.-D.; Russell, G. T.; Schmid, E. Initiator efficiencies in 2,2′-azoisobutyronitrile-initiated free-radical polymerizations of styrene. *Macromol. Chem. Phys.* **1994**, *195*, 2117−2140.
(44) Moad, G.; Rizzardo, E.; Thang, S. H. Radical addition−fragmentation chemistry in polymer synthesis. *Polymer* **2008**, *49*, 1079−1131.
(45) Moad, G.; Rizzardo, E.; Thang, S. H. Living Radical Polymerization by the RAFT Process - A Second Update. *Aust. J. Chem.* **2009**, *62*, 1402−1472.
(46) Keddie, D. J. A guide to the synthesis of block copolymers using reversible-addition fragmentation chain transfer (RAFT) polymerization. *Chem. Soc. Rev.* **2014**, *43* (2), 496−505.
(47) Monteiro, M. J.; Cunningham, M. F. Polymer Nanoparticles via Living Radical Polymerization in Aqueous Dispersions: Design and Applications. *Macromolecules* **2012**, *45*, 4939−4957.
(48) Zetterlund, P. B.; Thickett, S. C.; Perrier, S.; Bourgeat-Lami, E.; Lansalot, M. Controlled/Living Radical Polymerization in Dispersed Systems: An Update. *Chem. Rev.* **2015**, *115*, 9745−9800.
(49) Palivan, C. G.; Goers, R.; Najer, A.; Zhang, X. Y.; Car, A.; Meier, W. Bioinspired polymer vesicles and membranes for biological and medical applications. *Chem. Soc. Rev.* **2016**, *45* (2), 377−411.
(50) Pei, Y.; Lowe, A. B.; Roth, P. J. Stimulus-Responsive Nanoparticles and Associated (Reversible) Polymorphism via Polymerization Induced Self-assembly (PISA). *Macromol. Rapid Commun.* **2017**, *38*, 1600528.
(51) Tritschler, U.; Pearce, S.; Gwyther, J.; Whittell, G. R.; Manners, I. 50th Anniversary Perspective: Functional Nanoparticles from the Solution Self-Assembly of Block Copolymers. *Macromolecules* **2017**, *50*, 3439−3463.
(52) Penfold, N. J. W.; Yeow, J.; Boyer, C.; Armes, S. P. Emerging Trends in Polymerization-Induced Self-Assembly. *ACS Macro Lett.* **2019**, *8*, 1029−1054.
(53) Gurnani, P.; Perrier, S. Controlled radical polymerization in dispersed systems for biological applications. *Prog. Polym. Sci.* **2020**, *102*, 101209.
(54) Lefley, J.; Waldron, C.; Becer, C. R. Macromolecular design and preparation of polymersomes. *Polym. Chem.* **2020**, *11*, 7124−7136.
(55) Wong, C. K.; Qiang, X.; Muller, A. H. E.; Groschel, A. H. Self-Assembly of Block Copolymers into Internally Ordered Microparticles. *Prog. Polym. Sci.* **2020**, *102*, 101211.
(56) D'Agosto, F.; Rieger, J.; Lansalot, M. RAFT-Mediated Polymerization-Induced Self-Assembly. *Angew. Chem., Int. Ed.* **2020**, *59*, 8368−8392.
(57) Pearce, S.; Perez-Mercader, J. PISA: Construction of Self-Organized and Self-Assembled Functional Vesicular Structures. *Polym. Chem.* **2021**, *12*, 29−49.
(58) Gyorgy, C.; Armes, S. P. Recent Advances in Polymerization-Induced Self-Assembly (PISA) Syntheses in Non-Polar Media. *Angew. Chem., Int. Ed.* **2023**, *62*, No. e202308372.
(59) Baines, F. C.; Bevington, J. C. A Tracer Study of the Hydrolysis of Methyl Methacrylate and Methyl Acrylate Units in Homopolymers and Copolymers. *Polymer Chem.* **1968**, *6*, 2433−2440.

https://doi.org/10.1021/acs.macromol.4c01638
Macromolecules 2024, 57, 8983−8997